
Monotone 3D Finite Volumes and Andra 3D Test Case Modelling

Yuri Vassilevski and Ivan Kapyrin

Institute of Numerical Mathematics
Russian Academy of Sciences

Monotone Finite Volume Method: ideas

Introduced in 2D:

C. Le Potier. Schema volumes finis monotone pour des operateurs de diffusion fortement anisotropes sur des maillages de triangle non structures. C.C.Acad. Sci. Paris, Ser. I 341, pp.787-792, 2005.

Modified, also in 2D:

K. Lipnikov, M. Shashkov, D. Svyatski, Yu. Vassilevski. Monotone finite volume schemes for diffusion equations on unstructured triangular and shape-regular polygonal meshes. Journal of Computational Physics, Vol.227, No.1, pp.492-512, 2007.

Monotone Finite Volume Method in 3D

Model problem:

$$\begin{aligned}\nabla \cdot \vec{r} &= f, \\ \vec{r} &= -\mathcal{D}\nabla C \text{ p } \Omega, \\ C|_{\Gamma_D} &= g^D, \quad -\mathcal{D}\frac{\partial C}{\partial \vec{n}} \Big|_{\Gamma_N} = g^N.\end{aligned}\tag{1}$$

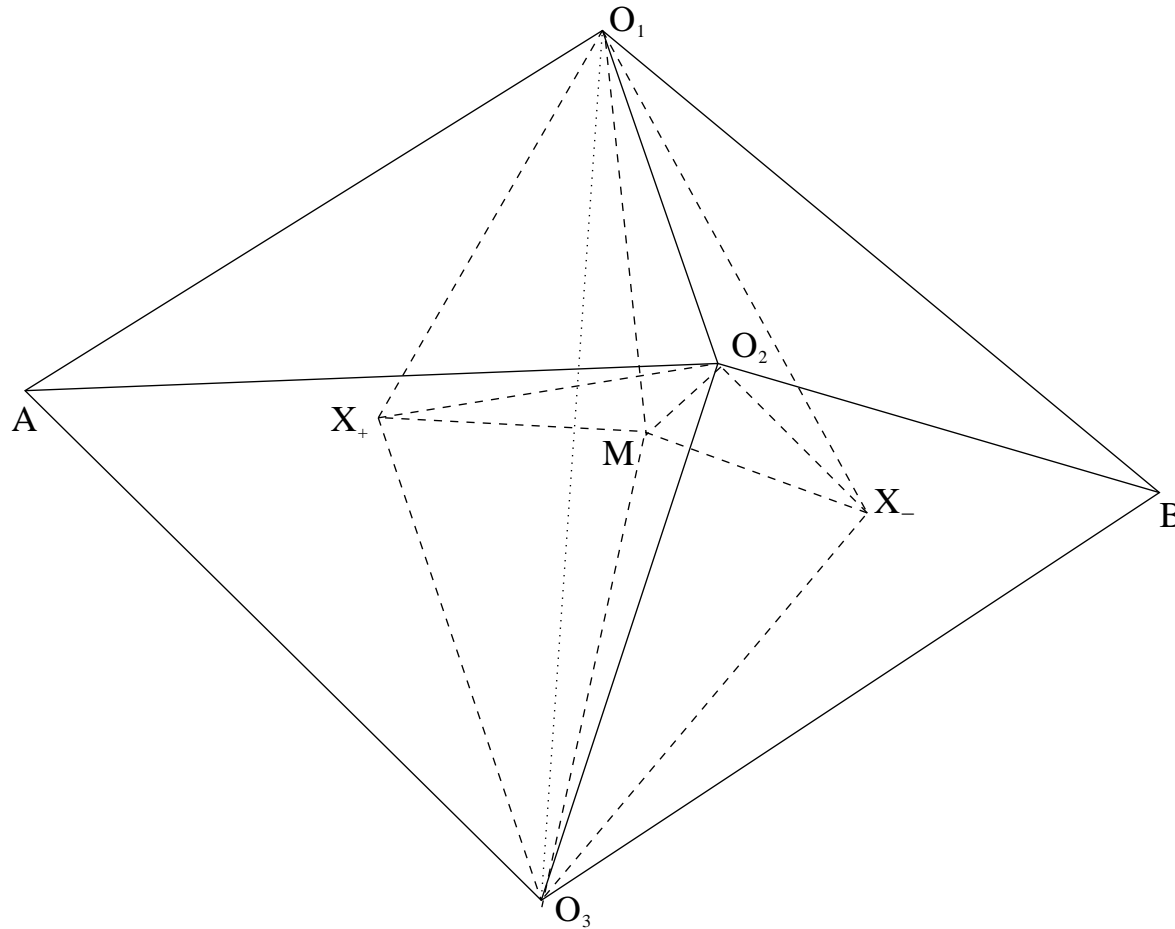
Conservation law:

$$\sum_{e \in \partial T} \vec{r}_e \cdot \vec{n}_e = \int_T f \, dx \quad \forall T \in \varepsilon_h,$$

Collocation point X_T for tetrahedron $T = ABCD$:

$$\vec{R}_{X_T} = \frac{\vec{R}_A \|\vec{n}_a\|_{\mathcal{D}} + \vec{R}_B \|\vec{n}_b\|_{\mathcal{D}} + \vec{R}_C \|\vec{n}_c\|_{\mathcal{D}} + \vec{R}_D \|\vec{n}_d\|_{\mathcal{D}}}{\|\vec{n}_a\|_{\mathcal{D}} + \|\vec{n}_b\|_{\mathcal{D}} + \|\vec{n}_c\|_{\mathcal{D}} + \|\vec{n}_d\|_{\mathcal{D}}}.$$

Geometrical constructions for VFMON



C_{X_+}, C_{X_-} - independent dimensions of freedom.

$C_{O_1}, C_{O_2}, C_{O_3}$ - expressed using C_X :
$$C_{O_i} = \sum_{j=1}^4 \lambda_{i,j} C_{X_{i,j}}.$$

Nonlinear approximation of the flux through a face

Linear combination:

$$\vec{r}_e \cdot \vec{n}_e = \mu_1^e \vec{r}_1^+ \cdot \vec{n}_e + \mu_2^e \vec{r}_2^+ \cdot \vec{n}_e + \mu_3^e \vec{r}_3^+ \cdot \vec{n}_e,$$

Apply the Green formula:

$$\int_T \mathcal{D}^{-1} \vec{r} dx = - \int_T \nabla C dx = - \int_{\partial T} C \vec{n} ds$$

$$\implies V_i^\pm \mathcal{D}_\pm^{-1} \vec{r}_i^\pm = \frac{1}{3} \left(\vec{n}_i^\pm C_{M,i} + \vec{n}_{ei}^\pm C_{X_\pm} + \vec{n}_{ij}^\pm C_{O_j} + \vec{n}_{ik}^\pm C_{O_k} \right).$$

$C_{M,i}$ are eliminated using the flux continuity condition:

$$\vec{r}_i^+ \vec{n}_e = \vec{r}_i^- \vec{n}_e$$

Definition of the coefficients in the flux approximation

- Preserve the approximation:

$$\sum_{j=1}^3 \mu_j^e = 1.$$

- Two-point stencil for the flux through a face approximation:

$$\vec{r}_e \cdot \vec{n}_e = K_+(\mathbf{C}_\mathbf{x})C_{X_+} - K_-(\mathbf{C}_\mathbf{x})C_{X_-}.$$

Parametric set of solutions:

$$\mu_1^e(p^e) = \mu_1^e(0) + p^e [C_{O_1}(a_{31} - a_{21}) + C_{O_2}a_{32} - C_{O_3}a_{23}],$$

$$\mu_2^e(p^e) = \mu_2^e(0) + p^e [C_{O_2}(a_{12} - a_{32}) + C_{O_3}a_{13} - C_{O_1}a_{31}],$$

$$\mu_3^e(p^e) = \mu_3^e(0) + p^e [C_{O_3}(a_{23} - a_{13}) + C_{O_1}a_{21} - C_{O_2}a_{12}].$$

If $\mu_i^e \geq 0$, $i \in \{1, 2, 3\}$, $\mathbf{C}_\mathbf{x} \geq 0$, then $K_+(\mathbf{C}_\mathbf{x}) > 0$ and $K_-(\mathbf{C}_\mathbf{x}) > 0$.

Nonlinear system and its properties

The resulting system of VFMON:

$$A(C_X)C_X = F.$$

Properties of matrix $A(C_X)$ (in case of non-negative C_X and μ_i^e):

1. Sparse structure (≤ 5 non-zero elements in a row).
2. $A_{ii}(C_X) > 0$, $A_{ij}(C_X) \leq 0 \quad \forall i, j$.
3. Strict diagonal dominance in columns.

$A^T(C_X)$ is an M-matrix $\Rightarrow ([A(C_X)]^T)^{-1} \geq 0$
 $\Rightarrow A(C_X)$ is a monotone matrix,
i.e. if $A(C_X)x \geq 0$, then $x \geq 0$.

Solving the nonlinear problem and the monotonicity Theorem

The resulting system of VFMON: $A(C_X)C_X = F$.

Picard method: $A(C_X^k)C_X^{k+1} = F$.

$A(C_X^k)$ is a monotone matrix provided C_X^k is non-negative.

Theorem. Let the right-hand side f in the stationary diffusion problem (1) be non-negative in Ω , the boundary conditions $g^D(x) \geq 0$ on Γ_D and $g^N(x) \leq 0$ on Γ_N , the initial guess $(C_X^0)_i \geq 0$, and on every Picard iteration for any interior face e we choose $\mu_i^e \geq 0$, $i \in \{1, 2, 3\}$. Then all the iterative approximations of C_X are non-negative,

$$(C_X^k)_i \geq 0, \quad i = 1, \dots, N_T, \quad \forall k \geq 0.$$

I. Kapyrin. A family of monotone methods for the numerical solution of three-dimensional diffusion problems on unstructured tetrahedral meshes.

Doklady Mathematics, 2007, Vol.76, No. 2, pp. 734-738.

Application to non-stationary problems

$$\frac{\partial C}{\partial t} - \nabla \cdot \mathcal{D} \nabla C = f, \quad f \geq 0$$

Implicit scheme

$$\left(\frac{V}{\Delta t} + A(C_X^{n+1}) \right) C_X^{n+1} = \frac{V}{\Delta t} C_X^n + F^{n+1},$$

Picard method:

$$\left(\frac{V}{\Delta t} + A(C_X^{n+1,k}) \right) C_X^{n+1,k+1} = \frac{V}{\Delta t} C_X^n + F^{n+1}, \quad k = 1, 2, \dots, \quad C_X^{n+1,0} = C_X^n.$$

Corollary 1. If $\mu_i^e \geq 0 \quad \forall e, i$, then $(C_X^{n+1,k})_j \geq 0, \quad j = 1, \dots, N_T, \quad k = 1, 2, \dots$

Application to non-stationary problems

$$\frac{\partial C}{\partial t} - \nabla \cdot \mathcal{D} \nabla C = f, \quad f \geq 0$$

Explicit scheme

$$\frac{V}{\Delta t} C_X^{n+1} = \left(\frac{V}{\Delta t} - A(C_X^n) \right) C_X^n + F^{n+1},$$

Corollary 2. Non-negativity of the solution C_X^{n+1} can be achieved by using a sufficiently small Δt , ensuring $(V/\Delta t - A(C_X^n))_{ii} \geq 0 \quad \forall i$.

Advantages and drawbacks of 3D VFMON

Advantages:

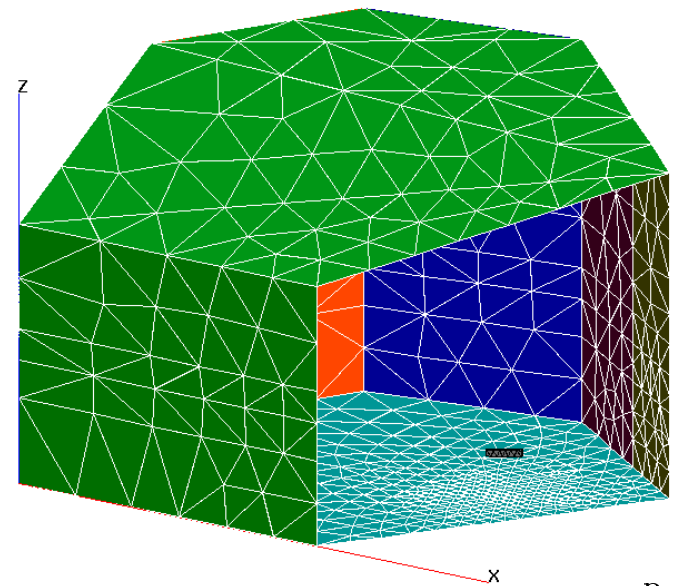
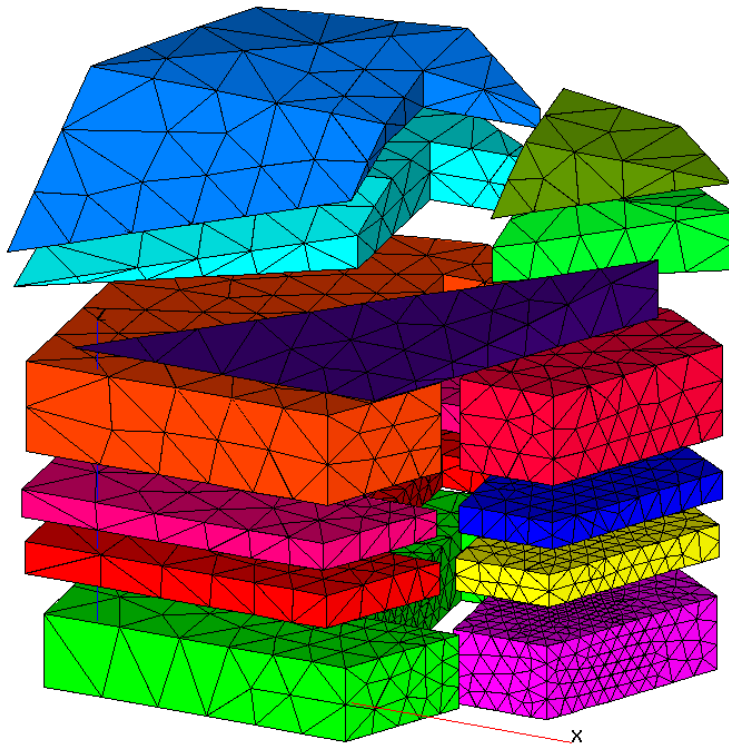
1. Local conservativity.
2. Non-negativity of solution.
3. 2-nd order of accuracy for the concentrations and 1-st order for the fluxes.

Drawbacks:

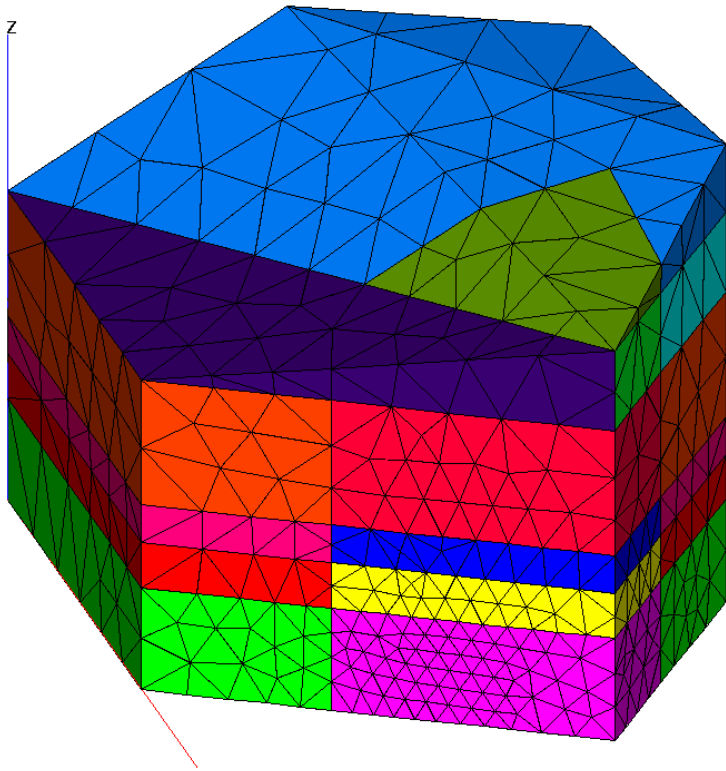
1. Convergence of Picard method can't be guaranteed.
2. More expensive than the conventional methods (about 20% slow-down with respect to the HMFEM method).
3. Problems with Neumann boundaries.

The Andra 3D Test Case

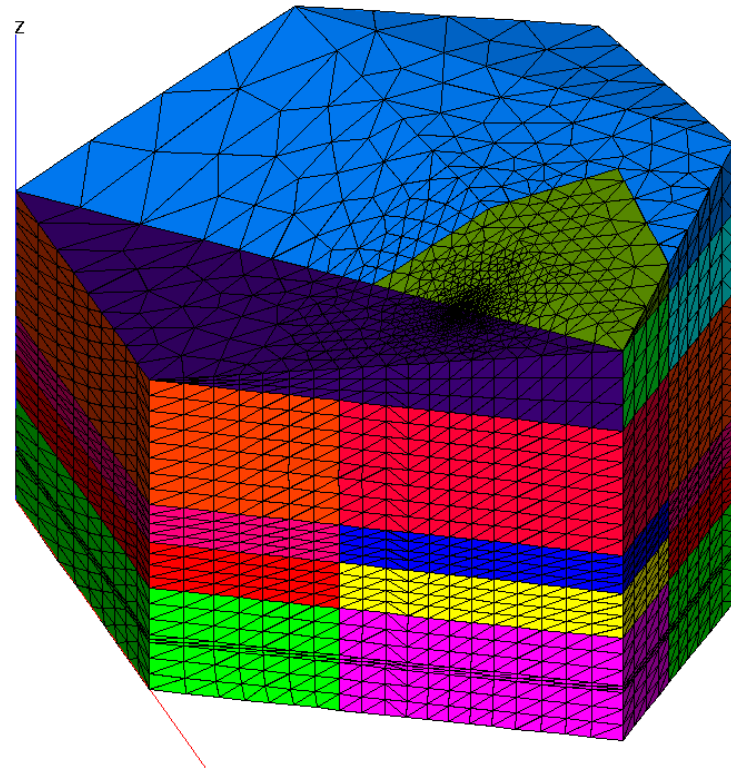
- Nonhomogeneity $\sim 10^{10}$ and anisotropy $\sim 10^2$ in the permeability tensor.
- Pinch-outs.
- Small thickness of the layers compared to the diameter of the domain.
- Full heterogeneous ($\sim 10^5$) diffusion tensor.



Computational grids

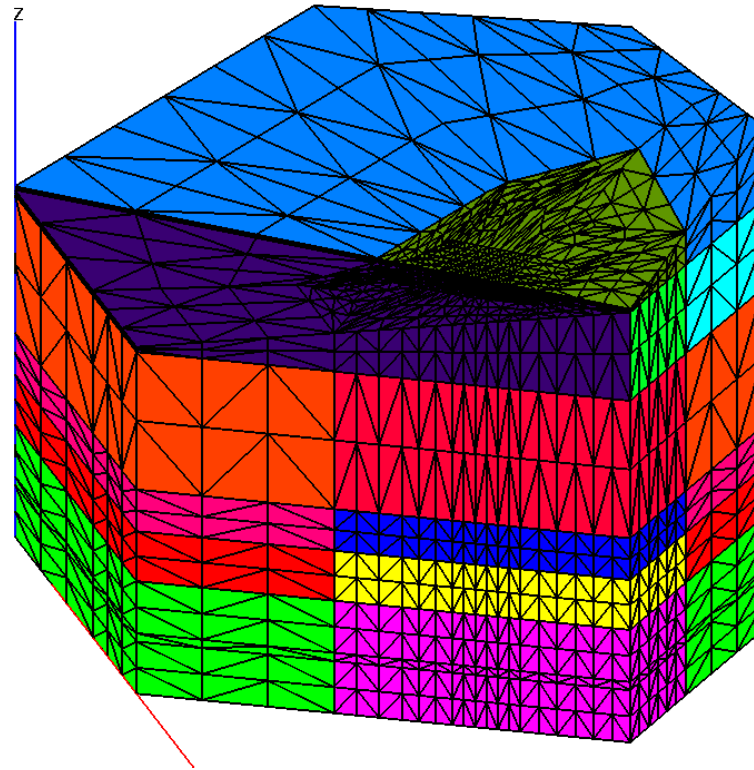


Completely unstructured grid.



Grid based on
triangular prisms splitting.

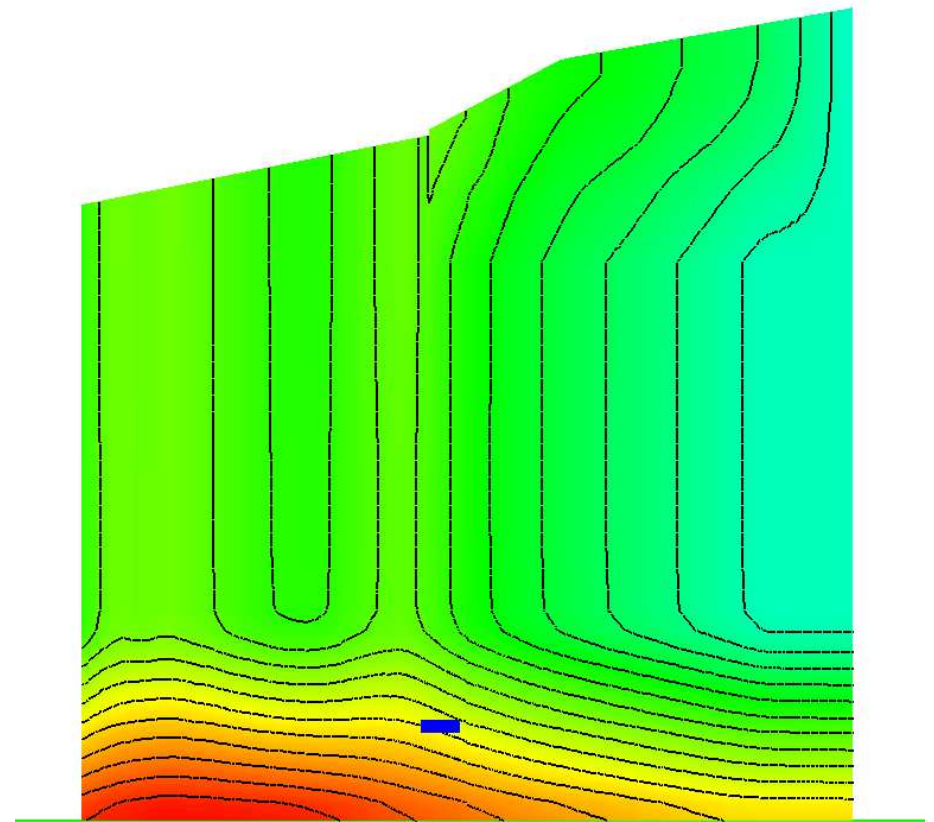
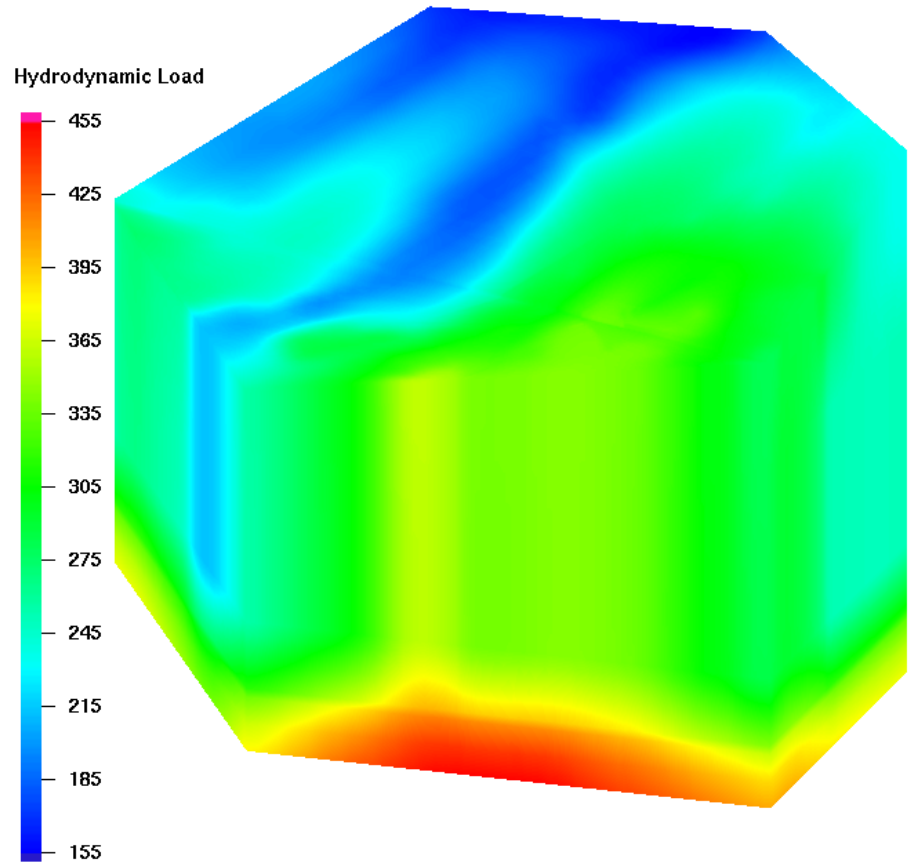
Computational grids



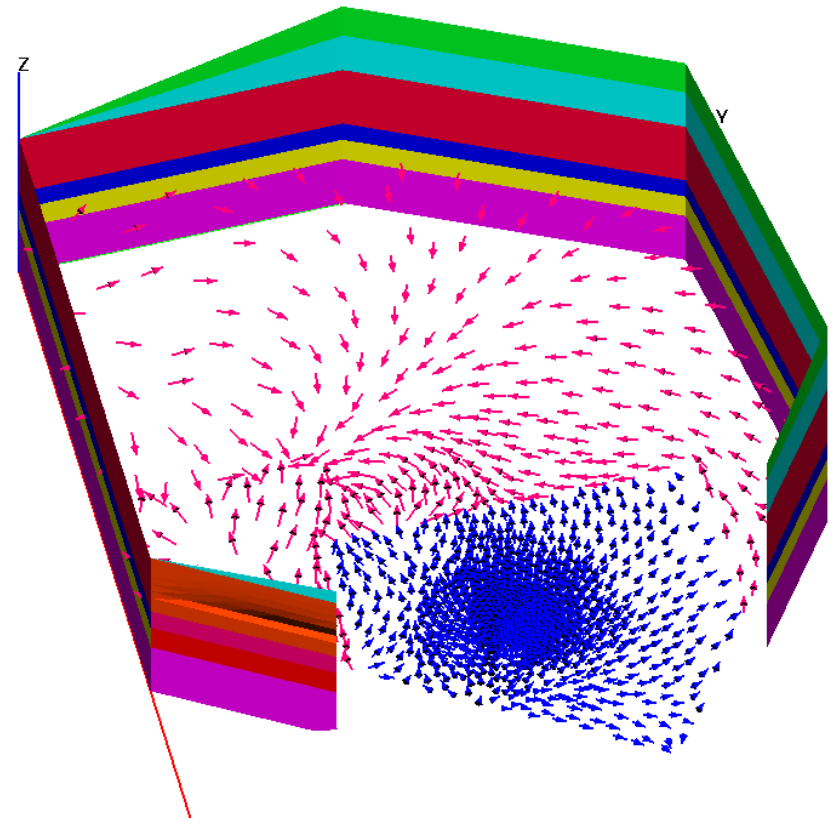
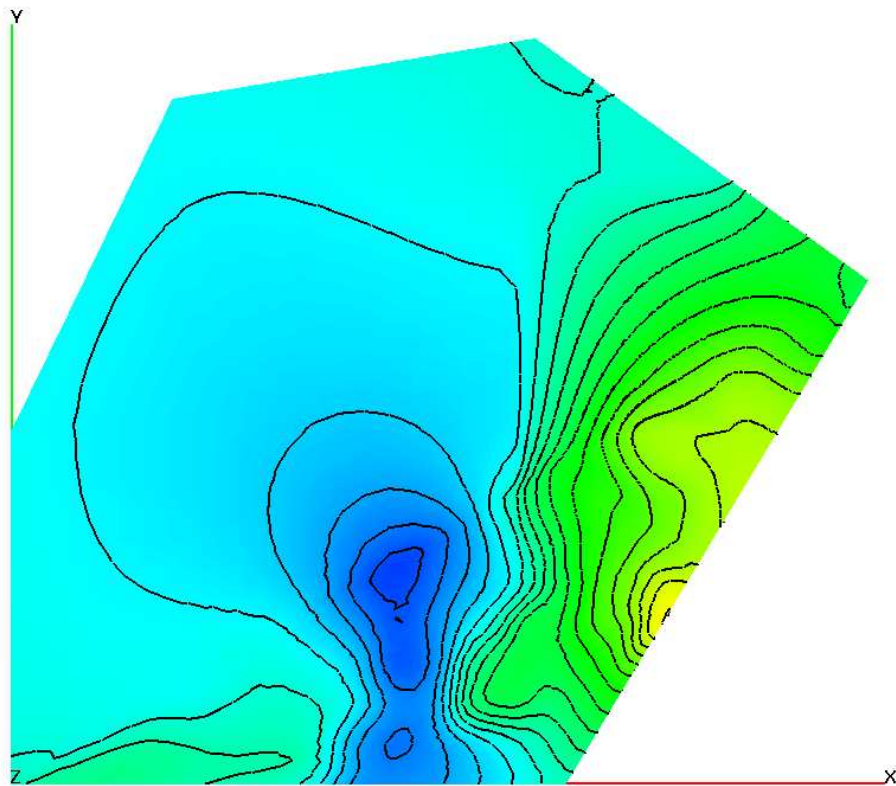
Grid based on splitting of hexahedrons and further local refinement.

The final mesh contains 2.5 mlns of tetrahedrons (5 mlns of unknowns in the linear systems)

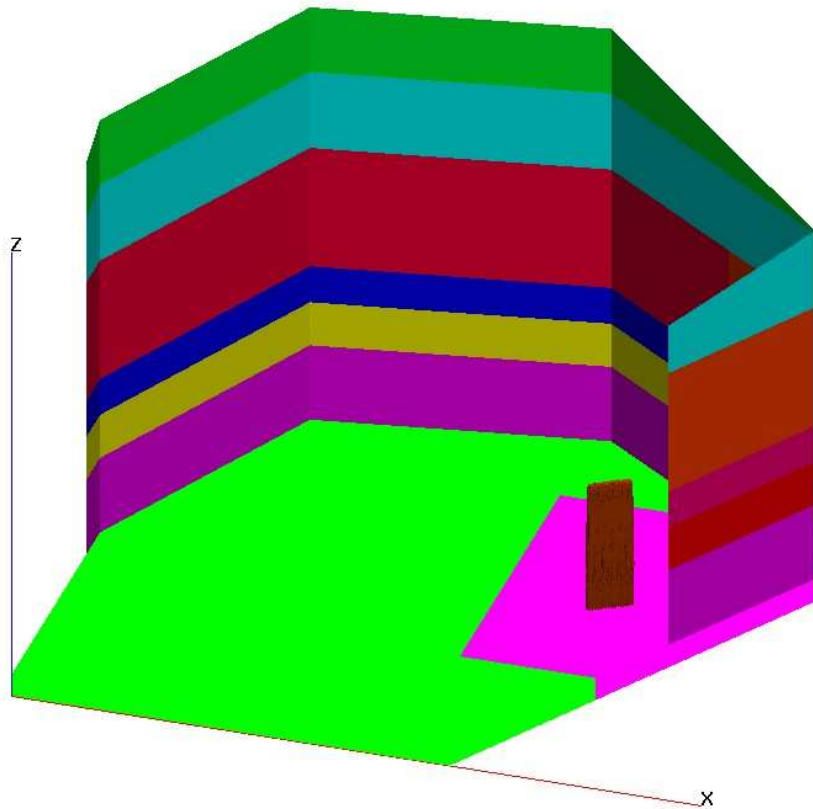
The results of hydrodynamic load calculations



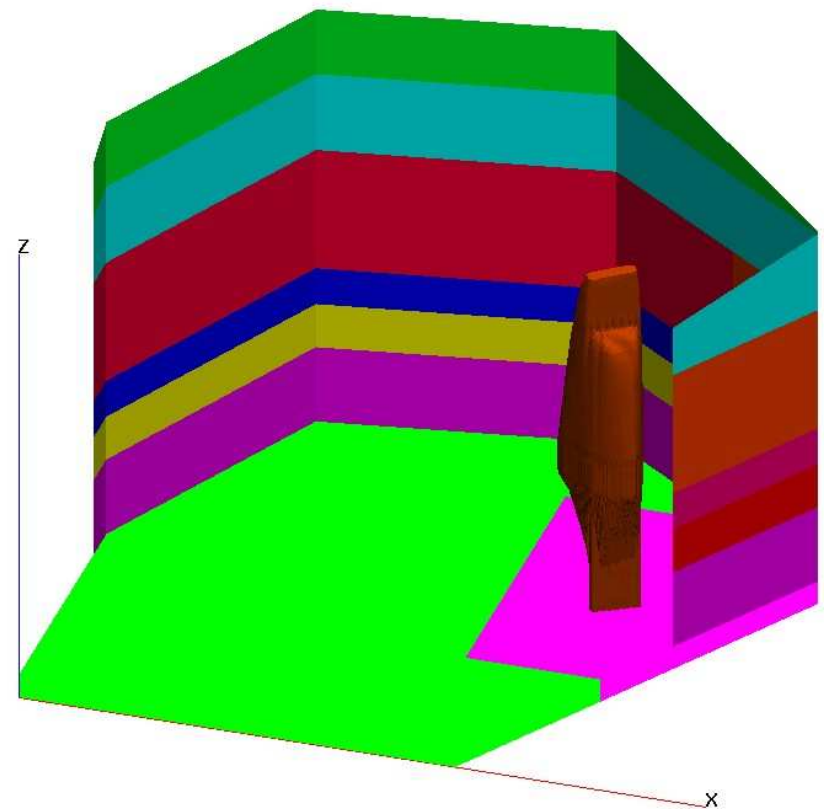
Results of advective fluxes calculation



Results: isosurface $C = 10^{-14}$

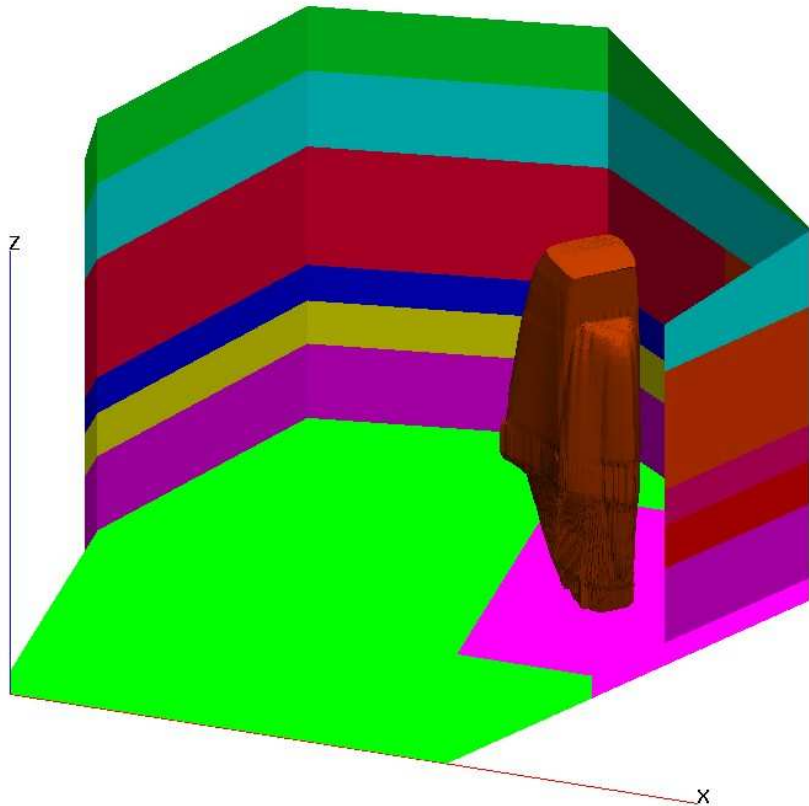


$T=10000$ years

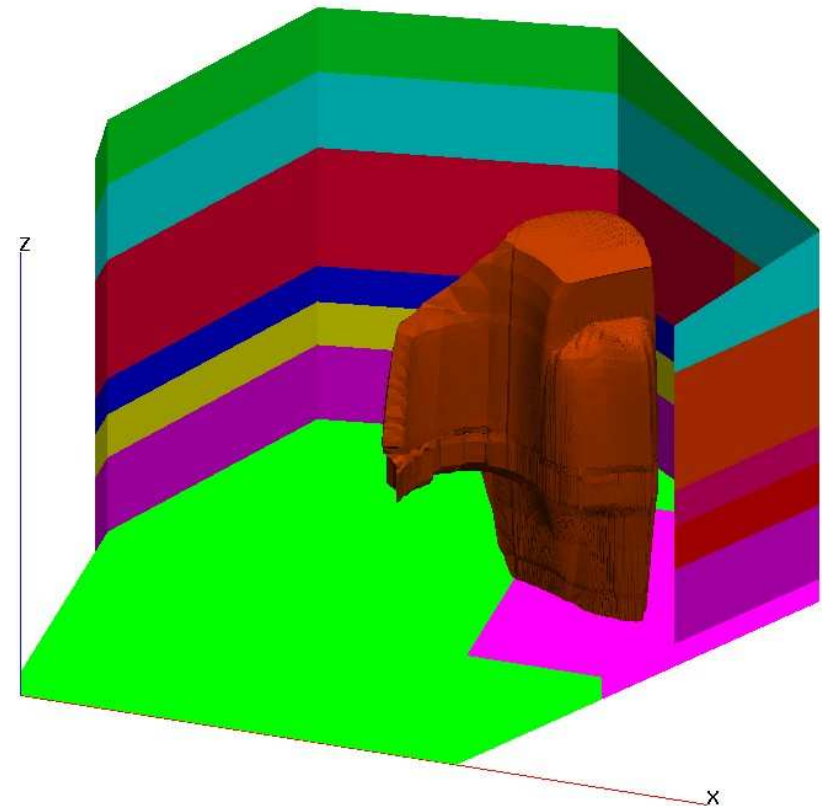


$T=50000$ years

Results: isosurface $C = 10^{-14}$

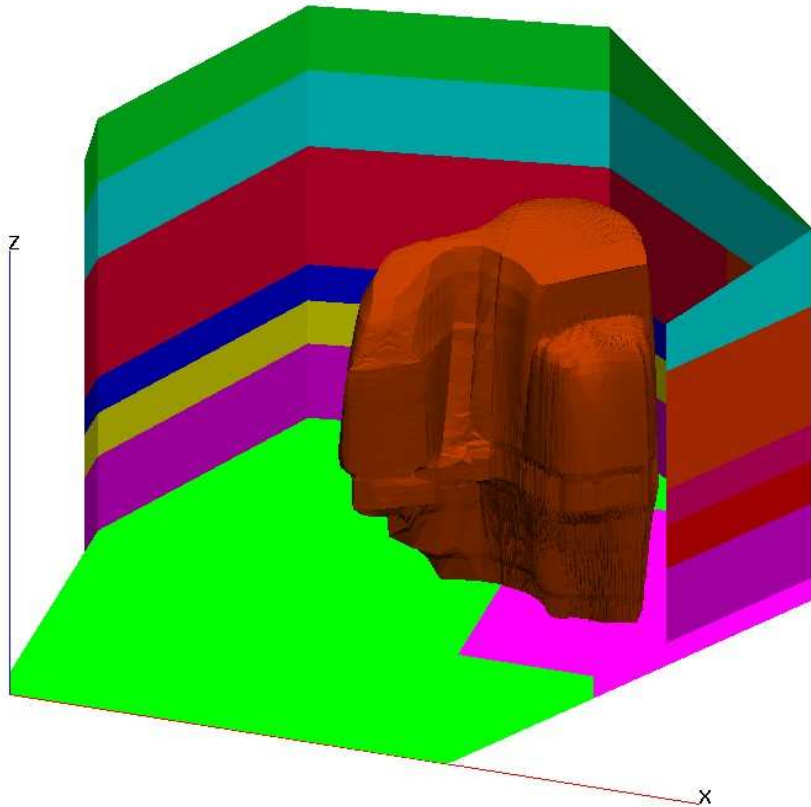


$T = 100000$ years

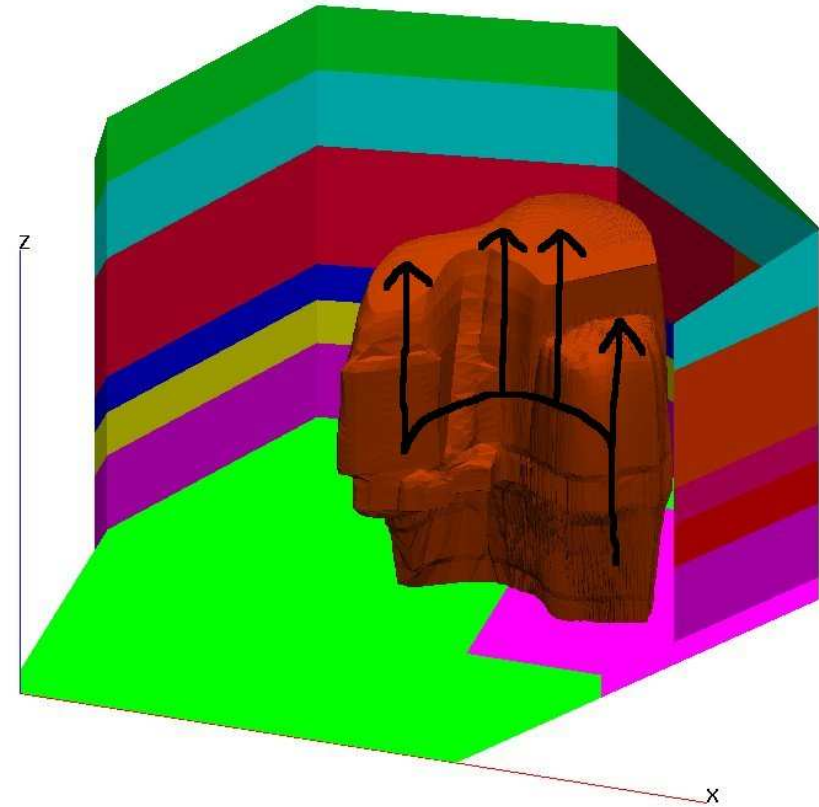


$T = 200000$ years

Results: isosurface $C = 10^{-14}$

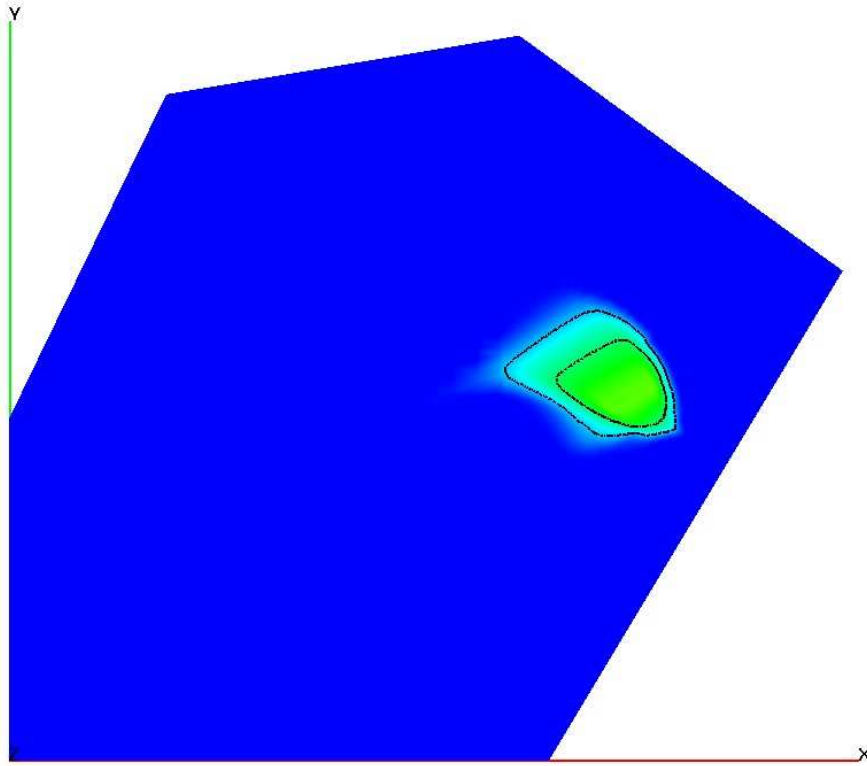


$T=300000$ years

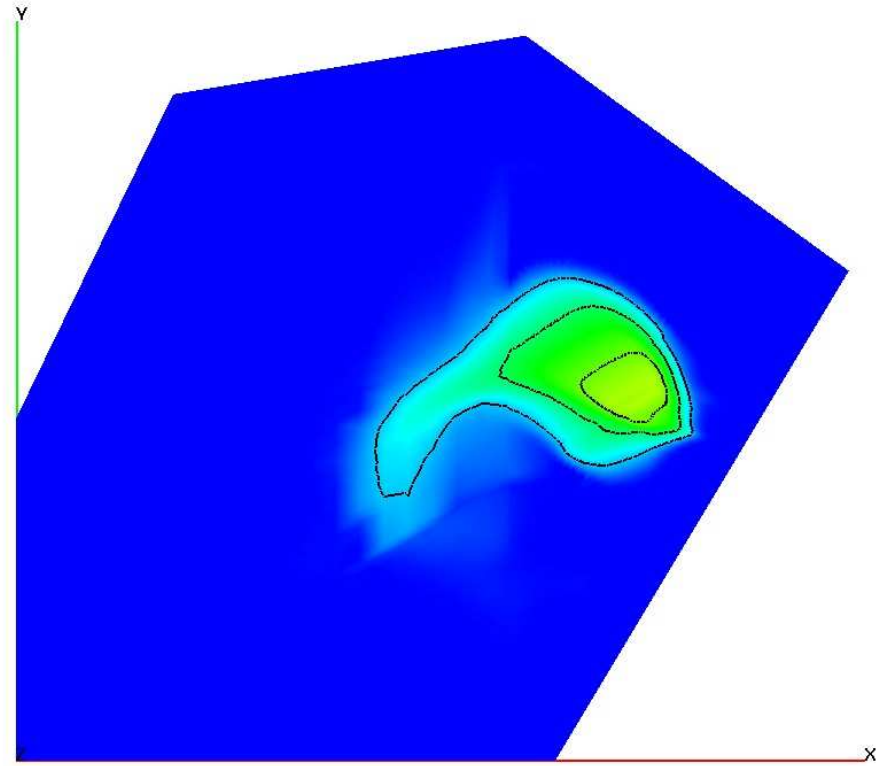


$T=350000$ years

Results: cross-section $Z = 35$

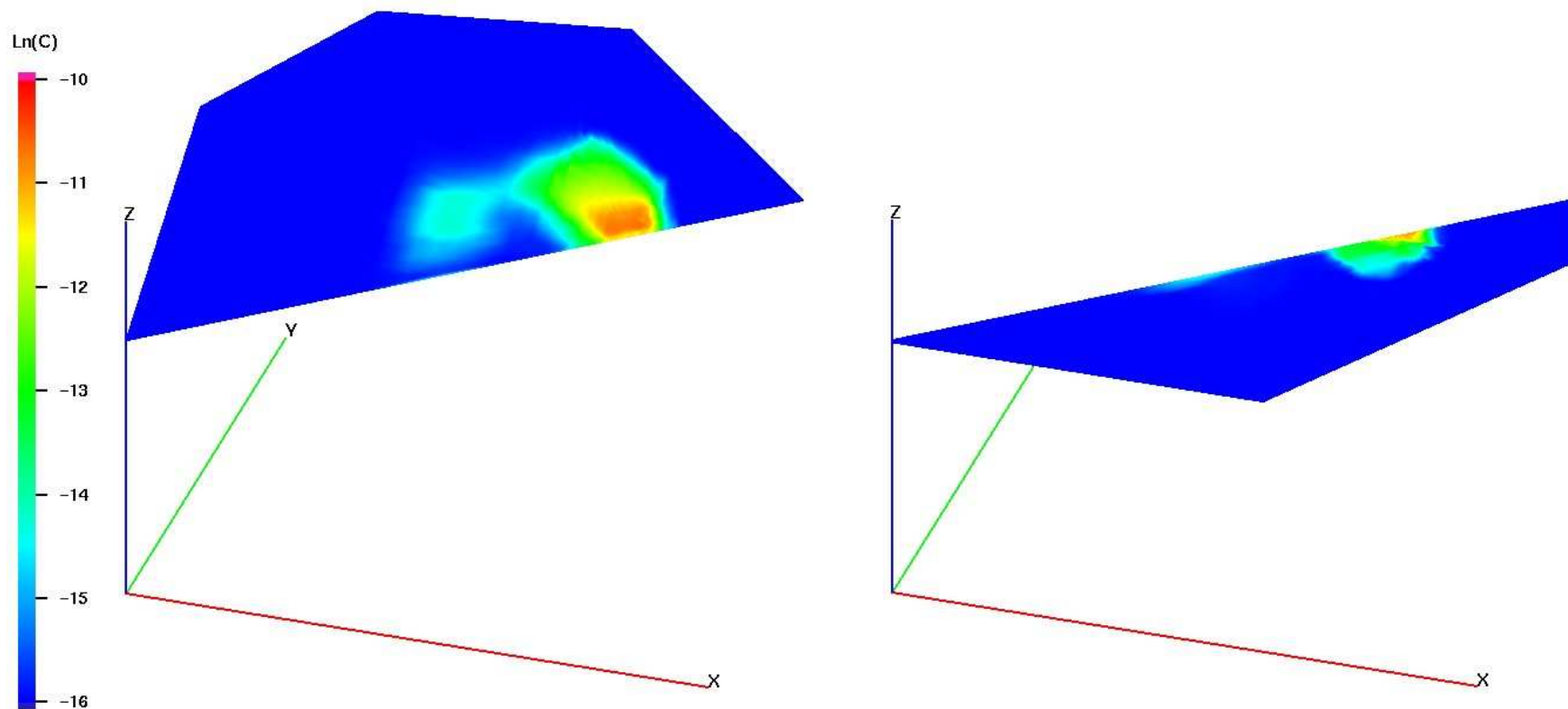


$T = 100000$ years



$T = 200000$ years

Results: pollution on the Earth surface



Solution in the uncovered layers (boundary conditions correspond to $T = 350000$ years): Tithonian (left) and Kimmeridgian not covered (right).